NUCLEAR THEORY, Vol. 39 (2022)
eds. M. Gaidarov, N. Minkov, Heron Press, Sofia

The Effect of Temperature on the Tidal Deformability of Neutron Stars

A. Kanakis-Pegios, P.S. Koliogiannis, Ch.C. Moustakidis

Department of Theoretical Physics, Aristotle University of Thessaloniki, 54124 Thessaloniki, Greece

Abstract. The recent detections of gravitational waves, which originated from binary neutron star mergers, offer a unique tool for studying the high-density region of dense nuclear matter. The role of temperature during the inspiral phase of a binary neutron star system is an open possibility, given the fact that there is not at this time evidence for its absence (zero temperature). Moreover, some theoretical studies suggest the existence of temperature, about a few MeV, during the last orbits before the merger. According to theory, friction may be developed in the star leading to the conversion of mechanical energy into heat. This effect might be detectable before the merger. In this work, our main purpose is to study the role of temperature on the tidal deformability of neutron stars, during the final stages of the inspiral phase. In our study, we used a variety of hot equations of state (isothermal and adiabatic) of various nuclear models. We found that for values of temperature below 1 MeV the tidal deformability as a relation to neutron star mass remains insensitive, though its ingredients (e.g. tidal Love number k_2) are affected. Regarding the adiabatic case, the thermal effect is unapparent up to $S = 0.2k_B$. This surprising behavior of tidal deformability is analyzed further.

1 Introduction

The detection of gravitational waves originated from binary black holes, binary neutron star and black hole-neutron star systems consists a very informative tool for physics [1, 2]. Especially, the entire process of a binary neutron star system is of great interest beacause it offers usefull insights on the properties of both cold and hot nuclear matter. In our study (for more details see Ref. [3]) we combined theoretical predictions and observational constraints through the tidal deformability [4–11].

According to theoretical statements, the temperature of a neutron star before the merger could be a few MeV [12–16]. Arras and Weinberg [17] suggested a main mechanism for the conversion of the mechanical energy into heat in the interior of a neutron star. Moreover, Meszaros and Rees [12] noticed that at the late phase of the inspiral of a coalescing binary neutron star system, the tidal effects can lead to a heat. Other studies found similar results [13, 14], while a relevant discussion has been given recently [15, 16].

Various studies suggested the presence of tidal heating effects, regardless the source that causes it [18–20]. Additionally, the meltdown of the crust during the inspiral phase has been studied in Ref. [21].Moreover, an inclusive study on the heat blanketing envelopes of neutron stars has been given in Ref. [22]. In general, the important role of the viscosity regarding neutron stars has been arised, affecting the heating of a a neutron star in an inspraling binary neutron star system. The predictions for the amount of heating focus in the following interval $T = 0.01 - 10$ MeV. The quantity of tidal deformability is very sensitive to the applied equation of state (EoS) of neutron stars. To be more specific, it depends on the tidal Love number k_2 and the star's radius R. Therefore, the study of the temperature effect in the tidal deformabiliy is of great interest, since the latter can be detected and constrained from the gravitational waves point of view.

The main idea that motivated our work was the study at which level the temperature affects the tidal deformability of a neutron star, during the inspiral phase of a binary neutron star system, just before the merger. In our study, we focused on the case of isothermal matter in the interior of neutron stars, employing various sets of EoSs, for temperatures in the range $T = 0.01 - 1$ MeV [23–27]. Details about the construction of hot EoSs can be found in Refs. [16, 28–34].

The fact that up until now there are no theoretical studies about the thermal effects on tidal deformability, led us to this study. The important role of the tidal deformability, as it connects the microscopic quantities of dense nuclear matter to the macroscopic quantities of neutron stars, emphasize this kind of study.

We notice that the study of the isothermal equilibrium of the star is not the most realistic. However, as a first order approach is more realisting than the cold star consideration. At the range of temperature that this study concentrated, the structure of the core of neutron stars is not affected too much. On the other hand, the crust is much more sensitive to the thermal effects. Nevertheless, in the mass range that is mainly measured from gravitational waves (1.2–1.6 $M_{\odot}$), the radius and therefore the tidal deformability, are quite sensitive to the structure and size of the crust. Furthermore, we extended our study to isentropic (adiabatic) EoSs for entropy $S < 1$, considering the neutron star to be in an adiabatic equilibrium.

The paper is organized as follows: In Section 2 we present the warm EoSs, where in Section 3, the basic theoretical backgound related to the tidal deformability is provided. The results, as well as their discussion, are explained in detail in Section 4. Finally, Section 5 contains the conclusions of the present work.

2 Warm Neutron Star Matter

The EoSs for the interior of neutron stars at finite temperature, as well as entropy per baryon, use the study of Koliogiannis and Moustakidis [27], where the data for the energy per particle for the symmetric nuclear matter and pure neutron matter, regarding the APR-1 EoS [35], and the momentum-dependent

interaction model are employed. To be more specific, the aforementioned parameterization is applied for the construction of three isothermal EoSs with $T = [0.01, 0.1, 1]$ MeV in a beta equilibrium state, and three isentropic EoSs with $S = [0.1, 0.2, 0.5]$ and proton fraction $Y_p = 0.2$.

2.1 Core of neutron stars

By taking into consideration the absence of neutrinos in adiabatic EoSs (to simulate the increment of temperature due to merger), in both profiles, isothermal and adiabatic, the exact relation for the chemical potentials μ_i, $i = \{e, p, n\}$ is

$$\mu_e = \mu_n - \mu_p = 4I(n,T)\left[F(n,T,I=1) - F(n,T,I=0)\right], \tag{1}$$

where $F(n,T,I)$ is the free energy per particle, and $I = 1-2Y_p$ is the asymmetry parameter, assuming that the EoS contains protons, neutrons, and electrons.

We notice that the calculation of the proton fraction in isothermal profile is possible through the beta equilibrium state, the Eq. (1), and the density of electrons defined as

$$n_e = \frac{2}{(2\pi)^3}\int \frac{d^3k}{1+\exp\left(\frac{\sqrt{\hbar^2k^2c^2+m_e^2c^4}-\mu_e}{T}\right)}. \tag{2}$$

However, in adiabatic profile, we consider that the proton fraction is almost constant. The energy density and pressure for the core of neutron stars, are constructed as

$$\mathcal{E}(n,T,I) = \mathcal{E}_b(n,T,I) + \mathcal{E}_e(n,T,I), \tag{3}$$

$$P(n,T,I) = P_b(n,T,I) + P_e(n,T,I). \tag{4}$$

Hence, Eqs. (3) and (4) constitute the ingredients for the EoSs in hot nuclear matter.

2.2 Crust of neutron stars

In both isothermal and adiabatic profiles, the EoSs for the region of the crust ($n_b < 0.08$ fm^{-3}) are given by the tabulated EoSs with finite temperature from StellarCollapse [1]. Especially, in isothermal profile, for the crust region we employed the EoSs of Lattimer and Swesty [23]. In all cases, the proton fraction of the crust remains constant, $Y_p = [0.1, 0.2, 0.3]$, leading to a total of nine EoSs. In adiabatic profile, for the crust region we employed the EoSs of Lattimer and Swesty [23] and Shen *et al.* [24]. In this case, the proton fraction matches the one of the core EoS, leading to a total of six EoSs.

Also, for reasons of completeness, we employed the EoSs of Lattimer and Swesty [23], Shen *et al.* [24], Banik *et al.* [25], and Steiner *et al.* [26] at full range. The Lattimer and Swesty [23] EoS is applied in $T = [0.01, 0.1, 1, 5, 10]$ MeV, while the remaining ones, are applied in $T = [0.01, 0.1, 1]$ MeV. For the total of 14 EoSs the proton fraction is constant, $Y_p = 0.1$.

[1] https://www.stellarcollapse.org

3 Tidal Deformability

The gravitational waves originated from the late phase of the inspral of a coalescing binary neutron star system are an important source for the detectors and lead to the estimation of various properties [36–38]. In this phase, the tidal effects are detectable [37].

We notice that the tidal Love number k_2, which depends on the EoS, describes the response of a neutron star to the presence of the tidal field E_{ij} [37]. The exact relation is the following:

$$Q_{ij} = -\frac{2}{3} k_2 \frac{R^5}{G} E_{ij} \equiv -\lambda E_{ij}, \tag{5}$$

where R is the neutron star radius and $\lambda = 2R^5 k_2/3G$ is the tidal deformability. The tidal Love number k_2 is given by [37, 38]

$$\begin{aligned} k_2 = {} & \frac{8\beta^5}{5} (1-2\beta)^2 [2 - y_R + (y_R - 1)2\beta] \\ & \times \Big[2\beta (6 - 3y_R + 3\beta(5y_R - 8)) \\ & + 4\beta^3 \left(13 - 11y_R + \beta(3y_R - 2) + 2\beta^2(1 + y_R)\right) \\ & + 3(1-2\beta)^2 [2 - y_R + 2\beta(y_R - 1)] \ln(1 - 2\beta) \Big]^{-1} \end{aligned} \tag{6}$$

where $\beta = GM/Rc^2$ is the compactness of a neutron star. The quantity y_R is determined by solving the following differential equation

$$r \frac{dy(r)}{dr} + y^2(r) + y(r)F(r) + r^2 Q(r) = 0, \tag{7}$$

with the initial condition $y(0) = 2$ [39]. $F(r)$ and $Q(r)$ are functionals of the energy density $\mathcal{E}(r)$, pressure $P(r)$, and mass $M(r)$ defined as [36]

$$F(r) = \left[1 - \frac{4\pi r^2 G}{c^4} (\mathcal{E}(r) - P(r))\right] \left(1 - \frac{2M(r)G}{rc^2}\right)^{-1}, \tag{8}$$

and

$$\begin{aligned} r^2 Q(r) = {} & \frac{4\pi r^2 G}{c^4} \left[5\mathcal{E}(r) + 9P(r) + \frac{\mathcal{E}(r) + P(r)}{\partial P(r)/\partial \mathcal{E}(r)}\right] \\ & \times \left(1 - \frac{2M(r)G}{rc^2}\right)^{-1} - 6\left(1 - \frac{2M(r)G}{rc^2}\right)^{-1} \\ & - \frac{4M^2(r)G^2}{r^2c^4} \left(1 + \frac{4\pi r^3 P(r)}{M(r)c^2}\right)^2 \left(1 - \frac{2M(r)G}{rc^2}\right)^{-2}. \end{aligned} \tag{9}$$

We notice that Eq. (7) has to be solved numerically and self consistently with the Tolman–Oppenheimer–Volkoff (TOV) equations using the boundary conditions

$y(0) = 2$, $P(0) = P_c$ (P_c denotes the central pressure), and $M(0) = 0$ [36,38]. The parameter y_R along with the compactness β are the basic ingredients of the tidal Love number k_2.

The chirp mass $\mathcal{M}_c$ of a binary neutron star system is a well constrained quantity by the detectors [1]. Its relation is given below

$$\mathcal{M}_c = \frac{(m_1 m_2)^{3/5}}{(m_1 + m_2)^{1/5}} = m_1 \frac{q^{3/5}}{(1+q)^{1/5}}, \tag{10}$$

where m_1 is the mass of the heavier component star and m_2 is the lighter's one. Therefore, the binary mass ratio $q = m_2/m_1$ lies within the range $0 \leq q \leq 1$.

Moreover, another quantity that is well constrained is the effective tidal deformability $\tilde{\Lambda}$ which is given by [1]

$$\tilde{\Lambda} = \frac{16}{13} \frac{(12q+1)\Lambda_1 + (12+q)q^4\Lambda_2}{(1+q)^5}, \tag{11}$$

where Λ_i is the dimensionless deformability [1]

$$\Lambda_i = \frac{2}{3} k_2 \left(\frac{R_i c^2}{M_i G} \right)^5 \equiv \frac{2}{3} k_2 \beta_i^{-5}, \quad i = 1, 2. \tag{12}$$

The effective tidal deformability $\tilde{\Lambda}$ is one of the main quantities that can be inferred by the detection of the corresponding gravitation waves.

4 Results and Discussion

The EoSs that we used in our study regarding the temperature effect on tidal deformability are based on the work of Ref. [27]. To be more specific, we follow the procedure of Ref. [27] for the construction of the core of the neutron star using the MDI+APR1 EoS, both for isothermal and adiabatic cases. We underline that the EoSs in both profiles contain only protons, neutrons, and electrons. For the crust region of isothermal neutron stars we employed the EoSs of Lattimer and Swesty [23], while for the adiabatic ones, we used the EoSs of Lattimer and Swesty [23] and Shen *et al.* [24]. In particular, in isothermal EoSs, the tabulated finite temperature EoSs contain entries up to $n_b = 10^{-13}$ fm^{-3}, which in this case, we consider to be the surface of the star ($n_{\rm surf}^{iso} = 10^{-13}$ fm^{-3}). On the contrary, in the adiabatic EoSs, since the desirable entropy per baryon can be found at various densities, we chose a common value, $n_b = 10^{-15}$ fm^{-3}, and extrapolate the EoSs for the crust until this value, i.e. $\log(n_b) - \log(\mathcal{E})$ and $\log(n_b) - \log(P)$. Therefore, the surface of the adiabatic EoSs is located at $n_{\rm surf}^{ise} = 10^{-15}$ fm^{-3}.

Specifically, we used the hot EoSs of Lattimer and Swesty [23], Shen *et al.* [24], Banik *et al.* [25], and Steiner *et al.* [26]. Also, we employed the MDI+APR1 EoS, which is suitable for the description of both cold and hot neutron star matter [27,40].

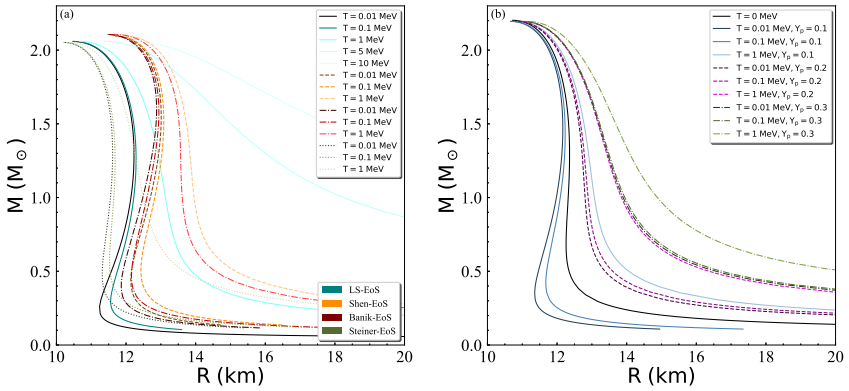

Figure 1. Mass-radius dependence for a) the four different nuclear models for various values of temperature and b) various values of temperature and proton fraction for the MDI+APR1 EoS. In panel a), the blue family of curves corresponds to the Lattimer and Swesty EoSs [23], the orange one to the Shen *et al.* EoSs [24], the red one to the Banik *et al.* EoSs [25], and the green one to the Steiner *et al.* EoSs [26].

In Figure 1 we show the mass-radius relation for a) the four different nuclear models and various values of temperature (the different line styles and family colors indicate the different models, while the higher temperature corresponds to the lighter color in each case; the same holds for the isothermal profile's figures) and b) the MDI+APR1 EoS for different values of temperature and proton fraction. In all cases the effect of the temperature is to increase the values of the radius (for a fixed value of mass). This effect is more clear at very high values of temperature. In addition, the increase of the proton fraction on the warm crust leads to the increase of the size of the neutron star, enhancing the effect of temperature.

In Figure 2 we show the temperature and proton fraction effects on the tidal parameters k_2, y_R, and λ for all nuclear models (top panel) and the MDI+APR1 EoS (bottom panel). As one can observe from the top panel of Figure 2, the increase of the value of temperature leads to a decrease in k_2, but simultaneously on an increase on y_R, for all EoSs. We underline that the latter parameter depends mostly on the neutron star structure. Although the radius and k_2 are sensitive to the temperature, the tidal deformability λ is not, as it is shown on the top panel in Figure 2c. We notice there is not any clear theoretical explanation for this kind of behavior. In the direction of exploring further this behavior, we observed that for values of temperature up to $T = 1\ MeV$ the product $\lambda \sim k_2 R^5$ holds.

Figure 2 (bottom panel) shows the effect of the proton fraction on λ. This effect is too small and it is present mainly on the very low mass region ($M \lesssim 1\ M_\odot$), which is out of interest in our study. Despite the differentiation of the EoSs in the panels a) and b) for the various values of proton fraction and tem-

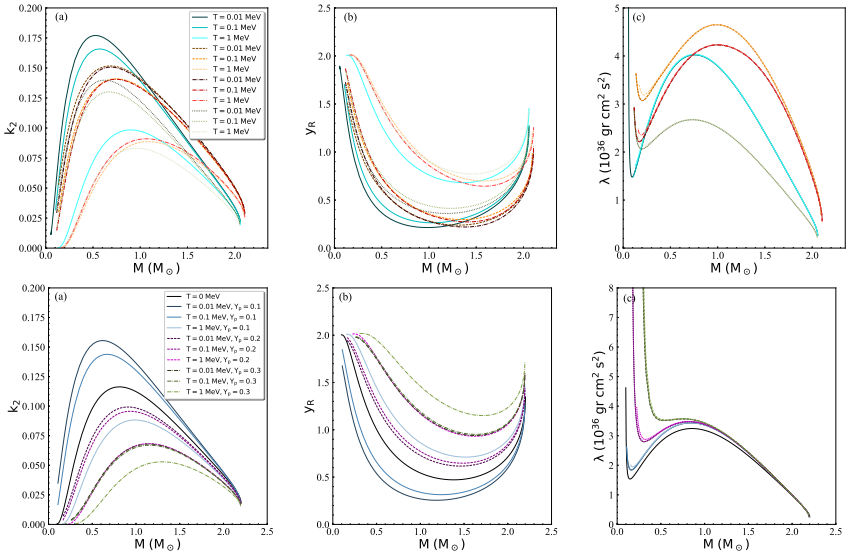

Figure 2. Thermal effects on the Love number k_2, parameter y_R, and individual tidal deformability λ for various values of temperature and for the four different nuclear models (top panel) and the MDI+APR1 EoS under different values of proton fraction [27] (bottom panel). The curves of diagrams b) and c) correspond to the legend of the diagram a), for each panel (top and bottom) respectively. The color of the curves on the top panel corresponds to those of the top panel of Figure 1.

perature, this behavior vanishes in the $\lambda - M$ diagram, leading the EoSs to be identical for high neutron star masses.

In Figure 3 we show the effect of the temperature and proton fraction on $\tilde{\Lambda}$ for the MDI+APR1 EoS, by using the binary neutron star mergers [1, 2]. In our study we adopted the proposed values for the chirp mass $\mathcal{M}_c$ and the component masses m_1, m_2 (under some minor modfication for the GW190425 event, so that $q \leq 1$) of both events. To be more specific, Figure 3a) corresponds to the GW170817 event while Figure 3b) corresponds to the GW190425 one. Similarly to the behavior of λ for a single neutrn star (see Figure 2c), all the EoSs have an identical behavior, except from the cold case. Moreover, the effect of the temperature is present mainly on the GW170817 event, which has lower component masses. Hence, binary neutron star systems with a low value of chirp mass $\mathcal{M}_c$ could be more suitable compared to binary neutron star systems with higher $\mathcal{M}_c$ such as the GW190415.

Moving further on the study of thermal effects on tidal deformability, we used a set of adiabatic EoSs under the consideration that the entropy per baryon is fixed. In that scenario, the gradient of the temperature is regulated to ensure constant entropy in the interior of the star. Especially, we employed two cases of adiabatic EoSs (according to the crust approach) with $S = [0.1, 0.2, 0.5]$.

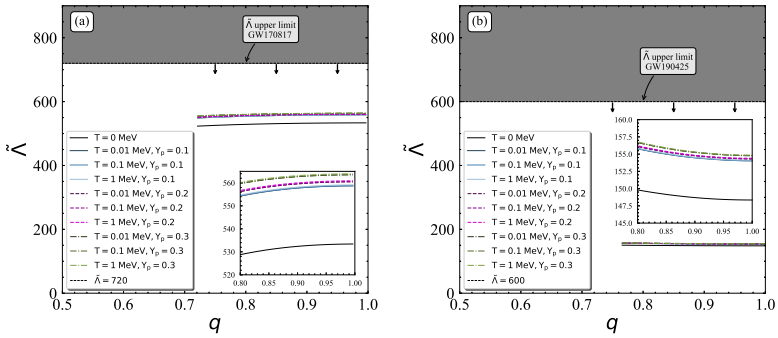

Figure 3. Thermal effects on $\tilde{\Lambda}$ as a function of the q for various values of temperature and proton fraction for the MDI+APR1 EoS and for the a) GW170817 and b) GW190425 event, respectively [1, 2]. The black curve corresponds to the cold EoS. The gray shaded regions indicate the measured upper limit on $\tilde{\Lambda}$ for each event.

Figure 4 represents the mass-radius diagram for the two EoSs and the three specific values of the entropy that we used in our study. The effect of temperature is insignificant for high neutron star masses. On the contrary, for lower masses, especially in the range we are interested, around $M = 1.4\ M_{\odot}$, there is an increase in the radius of the star as the temperature increases.

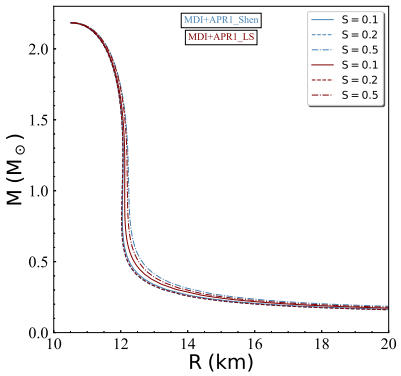

Figure 4. Mass-radius diagram for different values of S (in units of k_B) and for both crust considerations. The blue (red) curves indicate the Shen *et al.* [24] (Lattimer and Swesty [23]) crust approach, respectively.

Furthermore, in Figure 5 one can observe the effects of entropy on k_2, y_R, and λ. In more detail, the thermal effects are negligible on both k_2 and y_R, and consequently on λ. Specifically, the two set of EoSs lead to similar predictions for each value of the entropy (independently of the EoS) and depend mainly on the values of the entropy as displayed in Figure 5b).

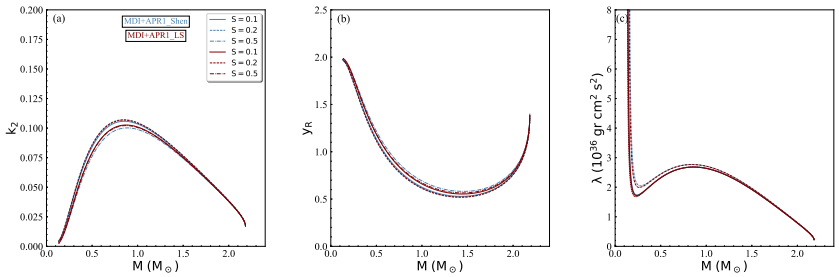

Figure 5. Entropy effects on tidal parameters, for both crust approaches. The blue (red) curves indicate the Shen *et al.* [24] (Lattimer and Swesty [23]) crust consideration. The curves of panels b) and c) correspond to the legend of the panel a).

5 Conclusions

According to our knowledge, up until now the thermal effects on the tidal deformability in the inspiral phase of a binary neutron star system have not been studied. Various studies suggest the presence of temperature of about a few MeV just before the merger. In our study, we explored how the temperature affects the tidal deformability, for both a single neutron star and a binary neutron star system, using the detections of binary neutron star mergers from the gravitational-waves point of view. The main finding is that even if the effect of temperature is important for k_2 and y_R parameters, this effect vanishes for the tidal deformability λ, for values of temperature up to $T < 1$ MeV. This fact is present regardless of the applied EoS. Therefore, it is very important to measure accurately the neutron star radius, so that useful insights can be gained regarding the temperature. In conclusion, we speculate that future detections of binary neutron star mergers could offer more information regarding the open question of the role of temperature.

Acknowledgments

We would like to thank Prof. P. Meszaros, Dr. S. Typel and Prof. D. Radice for their useful corresponds and suggestions. The research work was supported by the Hellenic Foundation for Research and Innovation (HFRI) under the 3rd Call for HFRI PhD Fellowships (Fellowship Number: 5657) and the State Scholarships Foundation (IKY) under Act number MIS 5113934.

References

[1] B.P. Abbott, et al., *Phys. Rev. X* **9** (2019) 011001.

[2] B.P. Abbott, et al., *Astrophys. J. Lett.* **892** (2020) L3.

[3] A. Kanakis-Pegios, P.S. Koliogiannis, Ch.C. Moustakidis, *Phys. Lett. B* **832** (2022) 137267.

[4] D. Radice, S. Bernuzzi, A. Perego, *Annu. Rev. Nucl. Part. Sci.* **70** (2020) 95119.
[5] L. Baiotti, *Progr. Part. Nucl. Phys.* **109** (2019) 103714.
[6] K. Chatziioannou, *Gen. Relativ. Gravit.* **52** (2020) 109.
[7] N. Sarin, P.D. Lasky, *Gen. Relativ. Gravit.* **53** (2021) 59.
[8] T. Dietrich, T. Hinderer, A. Samajdar, *Gen. Relativ. Gravit.* **53** (2021) 27.
[9] A. Kanakis-Pegios, P.S. Koliogiannis, Ch.C. Moustakidis, *Phys. Rev. C* **102** (2020) 055801.
[10] A. Kanakis-Pegios, P.S. Koliogiannis, Ch.C. Moustakidis, *Symmetry* **13** (2021) 183.
[11] P.S. Koliogiannis, A. Kanakis-Pegios, Ch.C. Moustakidis, *Foundations* **1(2)** (2021) 217-255.
[12] P. Meszaros, M.J. Rees, *Astrophys. J.* **397** (1992) 570.
[13] L. Bildsten, C. Cutler, *Astrophys. J.* **400** (1992) 175.
[14] C.S. Kochanek, *Astrophys. J.* **398** (1992) 234.
[15] E. R. Most, et al., *MNRAS* **509** (2022) 1096.
[16] A.Perego, S. Bernuzzi, D. Radice, *Europ. Phys. Journ. A* **55** (2019) 124.
[17] P. Arras, N.N. Weinberg, *MNRAS* **486** (2019) 1424.
[18] D. Lai, *MNRAS* **270** (1994) 611.
[19] A. Reisenegger, P. Goldreich, *Astrophys. J.* **426**, (1994) 688.
[20] W.C.G. Ho, D. Lai, *MNRAS* **308**, (1999) 153.
[21] Z. Pan, et al., *Phys. Rev. Lett.* **125**, (2020) 201102.
[22] M.V. Beznogov, A.Y. Potekhin, D.G. Yakovlev, *Phys Rep.* **919** (2021) 1-68.
[23] J.M. Lattimer, F.D. Swesty, *Nucl. Phys. A* **535** (1991) 331.
[24] G. Shen, C.J. Horowitz, S. Teige, *Phys. Rev. C* **83** (2011).
[25] S. Banik, M. Hempel, D. Bandyopadhyay, *Astrophys. J. Suppl. Ser.* **214** (2014) 22.
[26] A.W. Steiner, M. Hempel, T. Fischer, *Astrophys. J.* **774** (2013) 17.
[27] P.S. Koliogiannis, Ch.C. Moustakidis, *Astrophys. J.* **912** (2021) 69.
[28] J.M. Lattimer, M. Prakash, *Phys. Rep.* **621** (2016) 127-164.
[29] M.Prakash, et al., *Phys. Rep.* **280** (1997) 1-77.
[30] Ch.C. Moustakidis, C.P. Panos, *Phys. Rev. C* **79** (2009) 045806.
[31] J.B. Wei, et al., *Phys. Rev. C* **104**, (2021) 065806.
[32] S. Typel, *J. Phys. G: Nucl. Part. Phys.* **45** (2018) 114001.
[33] S. Typel, et al., *Phys. Rev. C* **81** (2010) 015803.
[34] T. Carreau, et al., *A&A* **635** (2020) A84.
[35] A. Akmal, V.R. Pandharipande, D.G. Ravenhall, *Phys. Rev. C* **82** (1998) 1804.
[36] S. Postnikov, M. Prakash, J.M. Lattimer, *Phys. Rev. D* **82** (2010) 024016.
[37] E.E. Flanagan, T. Hinderer, *Phys. Rev. D* **77** (2008).
[38] T. Hinderer, *Astrophys. J.* **677** (2008) 1216.
[39] T. Hinderer, et al., *Phys.Rev. D* **81** (2010) 123016.
[40] P.S. Koliogiannis, Ch.C. Moustakidis, *Phys. Rev. C* **101** (2020) 015805.